

Temperature-dependent Barkhausen volume in two-dimensional Ising-like ferromagnetic films

Qoimatul Mustaghfiroh,¹ Anabil Gayen ¹, Nguyen Le Thi ¹, Yunxiu Zhao,¹ Duy-Truong Quach ², Duc-The Ngo,³ Eunchong Baek,⁴ Chun-Yeol You ⁴, Yeon Suk Choi,⁵ Seung-Young Park,⁵ and Dong-Hyun Kim ^{1,*}

¹*Department of Physics, Chungbuk National University, Cheongju 28644, Korea*

²*Faculty of Basic Sciences, University of Transport and Communications, Hanoi 10000, Vietnam*

³*Department of Materials, University of Manchester M13 9PL, United Kingdom*

⁴*Department of Physics and Chemistry, DGIST, Daegu 42988, Korea*

⁵*Center for Scientific Instrumentation, Korea Basic Science Institute, Daejeon 34133, Korea*



(Received 29 August 2023; revised 28 March 2024; accepted 5 April 2024; published 23 April 2024)

We report our systematic investigation of temperature-dependent Barkhausen volume behavior for CoFeB/Pd with perpendicular magnetic anisotropy by means of magneto-optical Kerr microscopy. In the temperature range where two-dimensional (2D) Ising-like and single-domain features are sustained, hysteresis parameters such as coercivity, hysteresis area, and saturation magnetization are quantitatively analyzed with respect to the temperature. Interestingly it is demonstrated that the Barkhausen length is directly proportional to the domain-wall width via the magnetic anisotropy in this single-domain and 2D Ising-like model system.

DOI: [10.1103/PhysRevB.109.144419](https://doi.org/10.1103/PhysRevB.109.144419)

The thermal stability of physical systems is basically involved with competition between ordering interaction and disordering thermal agitation. In a ferromagnetic system, neighboring spins orderly form multiple magnetic domains divided by magnetic domain wall (DW), which plays a key role in magnetization reversal. Nowadays, one of the important technical issues is to accomplish ultrahigh-density and ultrafast operational spin devices, which require high thermal stability of a magnetic system [1–4]. Recently, the thermal stability of magnetic domains over wide temperature ranges has attracted fundamental interest since DW, an interface between differently directed magnetic domains, mimics ubiquitous interface dynamics observed in various physical systems such as fire front [5], wetting paper [6], superconductor phase fluctuation [7], and financial market fluctuation [8]. It has been well known that the statistical nature of DW dynamics in various systems is described by universality-class models such as an Ising model, depending on dimensionality and symmetry of systems [9–12].

In a ferromagnetic system, thermal stability is expressed by the ratio between the uniaxial magnetic anisotropy (K_u) multiplied by the volume (V) and the thermal energy ($k_B T$), given as $K_u V / k_B T$ [13]. $K_u V$ works as an energy barrier for magnetization reversal, providing a preferential direction of magnetization below the energy barrier. In a simple magnetic system with uniaxial magnetic anisotropy, the energy barrier is lowered by applying an external magnetic field due to the Zeeman energy. For magnetization to be aligned along an energetically preferred direction, the energy barrier should be overcome by thermal energy. Moreover, it is well known that thermal effect generally changes the hysteresis loop shape due

to changes in magnetic anisotropy and saturation magnetization in magnetic materials [14–16]. At elevated temperatures, for instance, a coercivity (H_c) of the hysteresis loop, roughly related to the magnetic anisotropy of the system, decreases [17], changing overall magnetization reversal behaviors.

Under external magnetic fields greater than H_c , magnetization reversal behavior is mediated by viscous damping mechanism [18] where thermal effect becomes less important due to the vanishing energy barrier. However, for external fields less than H_c , ferromagnetic systems are known to exhibit a thermally activated magnetization reversal behavior, overcoming an energy barrier [19]. DW velocity becomes ultraslow under much lower field, exhibiting a creep DW behavior [18,20–22], dominated by the disorders working as a pinning potential for magnetic DW. In this thermal regime, while overall magnetic DW characteristics are determined by the macroscopic magnetic energies and thermal energy, DW dynamics exhibits an interesting interface dynamic such as Barkhausen avalanches [10]. One of the important parameters in describing the DW dynamics in the thermal regime is a unit activation volume of magnetic materials, known as the Barkhausen volume [23]. The Barkhausen volume is believed to be mostly linked to the exchange-interaction length scale, while it has been reported that it is modified by magnetic anisotropy and disorders of systems as well [24]. It has been suggested that there exists a correlation between the Barkhausen volume and the temperature of magnetic systems [25,26], while no systematic explanation has been provided yet based on a universality class.

In this work, we report our comprehensive study to understand the temperature-dependent Barkhausen volume behavior in thermal activation regime of magnetization reversal, by correlating the major macroscopic magnetic properties such as coercivity, hysteresis loop area, and saturation magnetization, as well as DW patterns and universality class of

*Corresponding author: donghyun@chungbuk.ac.kr

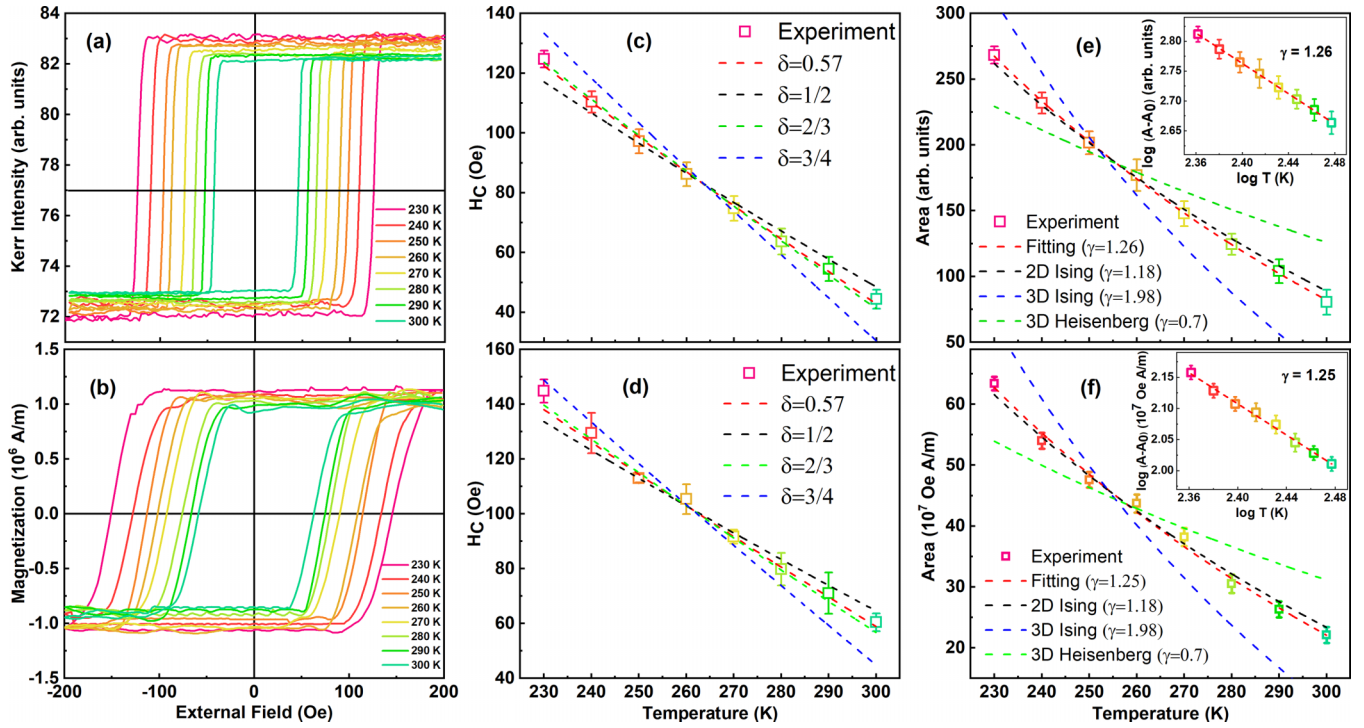


FIG. 1. Hysteresis loop measured by (a) MOKE measurement and by (b) VSM at different temperatures from 230 to 300 K with color codes. Coercivity (H_c) with respect to the temperature by (c) MOKE measurement with $\delta = 0.57 \pm 0.04$ and by (d) VSM with $\delta = 0.57 \pm 0.03$ with variation of temperature. Other δ values of 1/2 (black), 2/3 (green), and 3/4 (blue) are shown as dashed line. Hysteresis loop area measured by (e) MOKE with $\gamma = 1.26 \pm 0.11$ and by (f) VSM resulting $\gamma = 1.25 \pm 0.08$ (red dashed line). Inset $\log(A - A_0)$ vs $\log T$ with MOKE $\gamma = 1.26$ and VSM $\gamma = 1.25$. Hysteresis loop area fitted with various γ exponents from 2D Ising (black dashed), 3D Ising (blue dashed), and 3D Heisenberg (green dashed) models.

magnetization reversal with variation of temperatures. For a temperature range where a 2D Ising-like universal DW dynamics exists, it is observed that the Barkhausen volume is significantly changed with respect to the temperature, mainly determined by magnetic anisotropy.

Ta (2 nm)/Pd (2 nm)/[CoFeB (0.4 nm)/Pd (1 nm)]₄/Ta (1 nm) multilayer with a perpendicular magnetic anisotropy is deposited on Si(100) wafer substrate with a native oxide layer by dc magnetron sputtering. The detailed fabrication process is described elsewhere [16,27]. The thickness of the CoFeB sublayer was chosen to exhibit a strong perpendicular magnetic anisotropy. The multilayer films with repeat number of 6 and 8 were also prepared for comparison, where the domain patterns of multilayers with $n = 6$ and 8 are observed to be quite complex and jagged, not suitable for analysis of domain-wall velocity based on direct observation. Direct observation of temperature-dependent magnetic domain patterns and analysis of microscopic magnetic hysteresis loops were carried out by magneto-optical Kerr effect (MOKE) microscopy. After saturating the sample, a simple circular magnetic domain pattern is prepared by applying external fields of 58.7 Oe, for instance, at 270 K. After having circular domain with diameter of $\sim 360 \mu\text{m}$, the external field was turned off and then the temperature is changed to examine temperature-dependent domain patterns. Furthermore, at different temperatures, a circular domain is initiated by an applied field with proper strength to have almost the same size of the circular domain, to explore the DW velocity at each temperature. The domain images were processed by subtracting the background and

converted with black and white contrast. DW velocity was calculated at different temperatures (230–300 K) under different applied fields near the coercive field. MOKE hysteresis measurement per field and per temperature is repeated five times for all cases. Temperature-dependent saturation magnetization and magnetic anisotropy were measured by electromagnetic property measurement system developed in Korea Basic Science Institute.

MOKE hysteresis loop of the sample along the direction out of the film plane with variation of temperature in the range of 230–300 K is depicted in Fig. 1(a), where a perpendicular magnetic anisotropy at all temperatures is clearly confirmed. According to the MOKE microscopy observation, magnetization reversal is initiated with nucleation, and followed by subsequent DW motion. For comparison, we have further measured the magnetization hysteresis with magnetic moment directly measured by means of vibrating sample magnetometer (VSM), as demonstrated in Fig. 1(b). It should be mentioned that the shape of the hysteresis loop substantially changes from a fat to a narrow square as the temperature increases for both cases. The temperature-dependent coercivity from the MOKE microscopy observation is plotted in Fig. 1(c), where it is fitted by the law expressed in Eq. (1), known as Kneller's formula:

$$H_c(T) = H_0 \left[1 - \left(\frac{T}{T_B} \right)^\delta \right] \quad (1)$$

where H_0 is the coercivity at 0 K and T_B is the blocking temperature. δ is the exponent, involved with sample properties such as magnetic anisotropy and magnetic particle size [17,28,29]. For the present sample, $H_0 = 600$ Oe, matching well with previously reported values [30,31]. T_B is fitted to be 340 K, while the Curie temperature for the sample is 450 K. Since the sample has polycrystalline structure, T_B becomes more relevant in determination of the coercivity due to the disconnected granular behavior [32]. The fitting based on Eq. (1) gives the value of the exponent $\delta \sim 0.57 \pm 0.04$ for MOKE result. Temperature-dependent coercivity measured by VSM is found to be similar to $\delta \sim 0.57 \pm 0.03$, as shown in Fig. 1(d), consistent with the results from the MOKE microscopy. The MOKE measurement is a microscopic measurement carried out for $640 \times 480 \mu\text{m}^2$, while the VSM measurement is carried out over the whole sample with 1 cm^2 so that there might be difference in the loop slope and H_C . For systems which follow the single-domain model with uniaxial anisotropy noninteracting particles, it is reported that $\delta = 1/2$ [33]. For particles taking into account intraparticle interaction between domains, $\delta = 2/3$ [34], whereas for randomly oriented noninteracting particle, $\delta = 3/4$ [35]. The fitted δ value of the present sample is found to be close to the single-domain model value ($1/2$).

The temperature-dependent hysteresis loop area scaling observed by MOKE microscopy is plotted in Fig. 1(e), together with the loop-area scaling measured by VSM in Fig. 1(f). The hysteresis loop area decreases with increasing temperature, indicating that the energy loss, characterized by the hysteresis loop area, decreases with respect to the temperature. Since the coercivity as well as saturation magnetization decreases with respect to the temperature, the area should also decrease with respect to the temperature. In the inset of the figure, $\log(A - A_0)$ versus $\log T$ is plotted to confirm the power-law behavior. It is well known that the hysteresis loop area exhibits a scaling behavior, described as the Steinmetz law as $(A - A_0) \propto H_{\text{max}}^\alpha f^\eta T^{-\gamma}$, where A_0 is zero-temperature adiabatic loop area. α , η , and γ are the scaling exponents for the maximum field, frequency, and temperature, respectively [36]. There have been some available reports on α and η values but, for the γ exponent, only a few experimental results have been reported to date [37–40]. In the present study, the frequency ($f = 19.5$ Oe/s) and the maximum field ($H_{\text{max}} = 200$ Oe) were kept constant, only the temperature is varied to observe γ , focusing on thermal effect on energy loss during a hysteresis loop cycle, where experimental data have been simply fitted with the equation $(A - A_0) \propto T^{-\gamma}$. The fitted value of γ is found to be $\sim 1.26 \pm 0.11$ for MOKE result, again consistent with the VSM result of $\gamma = 1.25 \pm 0.08$. Interestingly, these values are close to theoretical prediction of 2D Ising model value (1.18) [41], while the model value of 3D Ising model and 3D Heisenberg model is 1.98 and $0.7 \sim 0.8$, respectively [37,41]. The γ value in the present study is significantly larger compared to the experimental report (~ 0.38) available for Permalloy films with in-plane magnetic anisotropy [38], which, in this case, was rather close to the theoretical model value (0.25) from the 2D Heisenberg model. Thus, it is considered that although there might be a little discrepancy between experimental results and the model, the CoFeB/Pd multilayer film with perpendicular magnetic

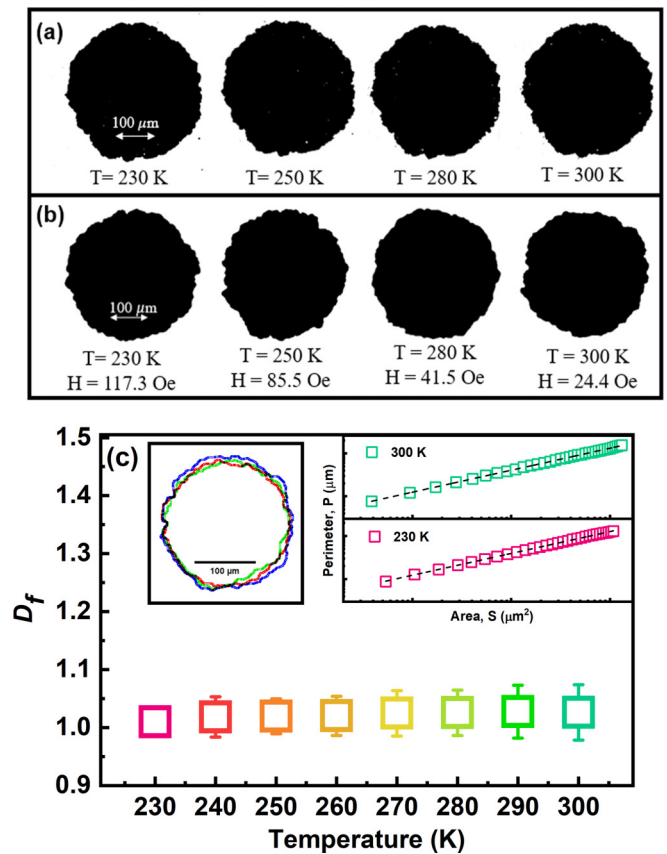


FIG. 2. Typical domain evolution pattern observed by MOKE microscopy at zero external field state at various temperatures. (a) Circular-shaped single domain initiated by external field, then observed with variation of temperatures. (b) Circular-shaped single domain prepared by proper external field at each temperature. (c) Fractal dimension (D_f) with respect to temperatures. Inset: superposition image of domain-wall boundary with three times measurement repetition and perimeter-area relation on log-log scale at 230 and 300 K.

anisotropy in the present study clearly exhibits the nature of the 2D Ising system for the temperature range of 230–300 K.

Corresponding domain images at various temperatures in Fig. 2(a) are recorded after positively saturating the sample and then applying negative fields near the coercivity. During the domain observation, the field is kept at 0 Oe to avoid any possible effect of the external field and thus, to visualize the temperature effect on the domain structure. It should be mentioned that as expected from the universality class of the 2D Ising nature in the temperature range, domain shape remains almost the same for 230–300 K. We have also checked the domain patterns, by applying proper external fields to have the same magnetization at different temperatures as demonstrated in Fig. 2(b). The external field is turned off when the amount of magnetization reversal reaches the same level as in Fig. 2(a) at each temperature. Again, almost the same domain pattern is observed, only with reduction of the required external-field strength to have a similar domain at elevated temperature, consistent with the δ value of the single-domain model, as observed in Fig. 1(b). The images are recorded by repeating three times and there exists microscopic fluctuation in the wall

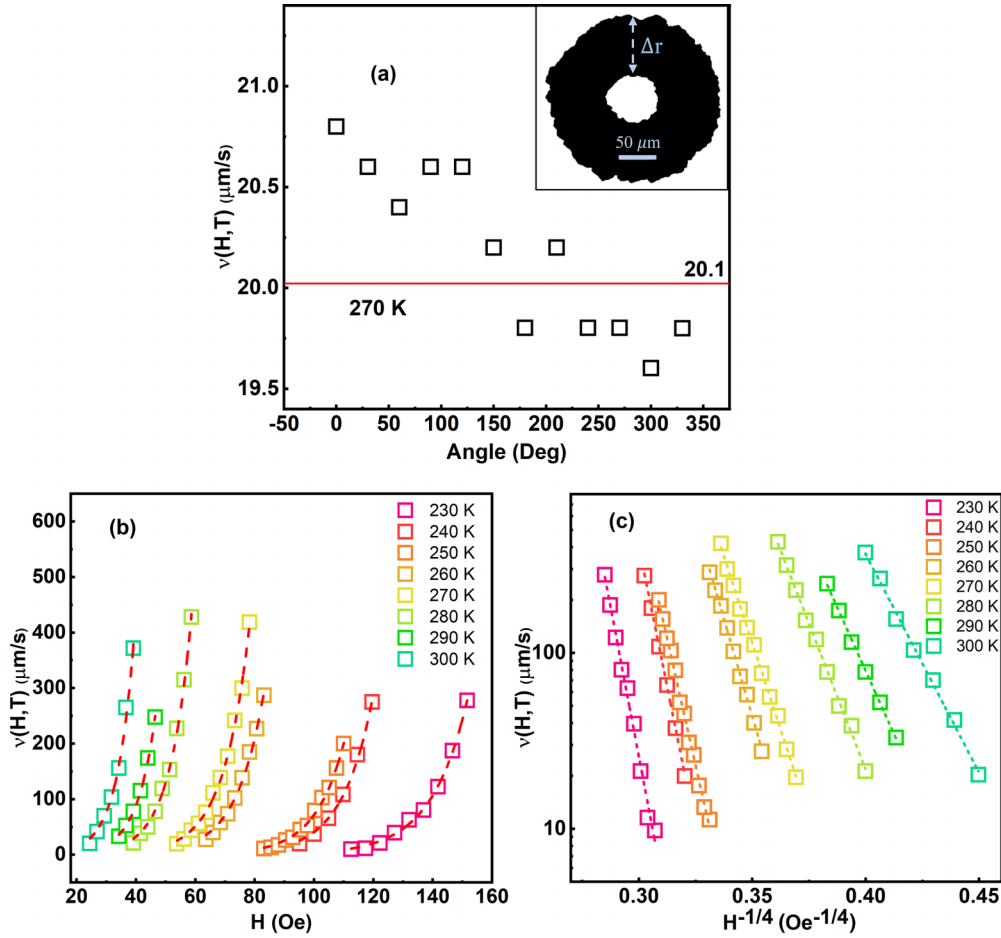


FIG. 3. (a) Domain displacement (Δr) at every 30° of circle domain at 270 K where the inset figure is circle domain configuration. (b) Domain-wall velocity, $v(H, T)$ vs applied magnetic field (H) at different temperatures, with fitting by the Arrhenius law (dashed line). (c) $v(H, T)$ vs $H^{-1/4}$ with linear fitting on a log-normal scale.

boundary, while the statistical nature of the DW pattern is sustained, as in the inset figure of Fig. 2(c). To quantitatively analyze the jaggedness of DW with change of temperature, the fractal dimension (D_f) of DW geometry is calculated by the perimeter (P)–area (S) scaling relation method, as depicted in Fig. 2(c). The linear relation between P and S on a log-log scale allows us to deduce the D_f from the slope of $P \propto S^{D_f/2}$, represented in the inset [42,43]. As expected from the direct domain-pattern observation, D_f is found to be almost 1 for the whole temperature range as seen in Fig. 2(c), clearly indicating that a simple linelike interface geometry of DW is persistently observed for the temperature range of 230–300 K without interface roughening by distributed random disorders.

Now, we further analyze the dynamic nature of the magnetic domains. DW velocity v is determined by quantitative analysis of time-dependent DW displacement with variation of external fields at each temperature, as depicted in Fig. 3. The v is first determined from angular averaging of circular domain expansion as seen in Fig. 3(a) and then repeated three times. Since the microscopic fluctuation and angular dispersion are well suppressed by the overall circular domain shape, it is considered that the averaging provides a representing value of v .

The v is exponentially increasing with the applied field at each temperature. The v is fitted with the Arrhenius equation, described in Eq. (2):

$$v(H, T) = v_0 \exp \left(- \frac{E - 2HM_s V_B}{k_B T} \right). \quad (2)$$

In Eq. (2), v_0 is the prefactor, E is activation energy proportional to the energy to overcome the barrier, H is an applied field, M_s is a saturation magnetization, V_B is a Barkhausen volume, and k_B is the Boltzmann constant [24]. The exponential behavior as a function of applied field at each temperature is a signature of thermally activated magnetization-reversal behavior. In the low-field regime, away from the coercive field, it has been known that the DW creep behavior is also observed. To verify the creep behavior for the present sample, we plot v versus $H^{-1/4}$ as in Fig. 3(b), where the creep exponent $\mu = 1/4$ is found to be valid for the whole temperature range of 230–300 K [44]. The universality class of creep exponent $\mu = 1/4$ is extensively observed for various two-dimensional ferromagnetic thin films with the perpendicular magnetic anisotropy [18]. Note that the creep exponent for the three-dimensional system is $1/2$ [45].

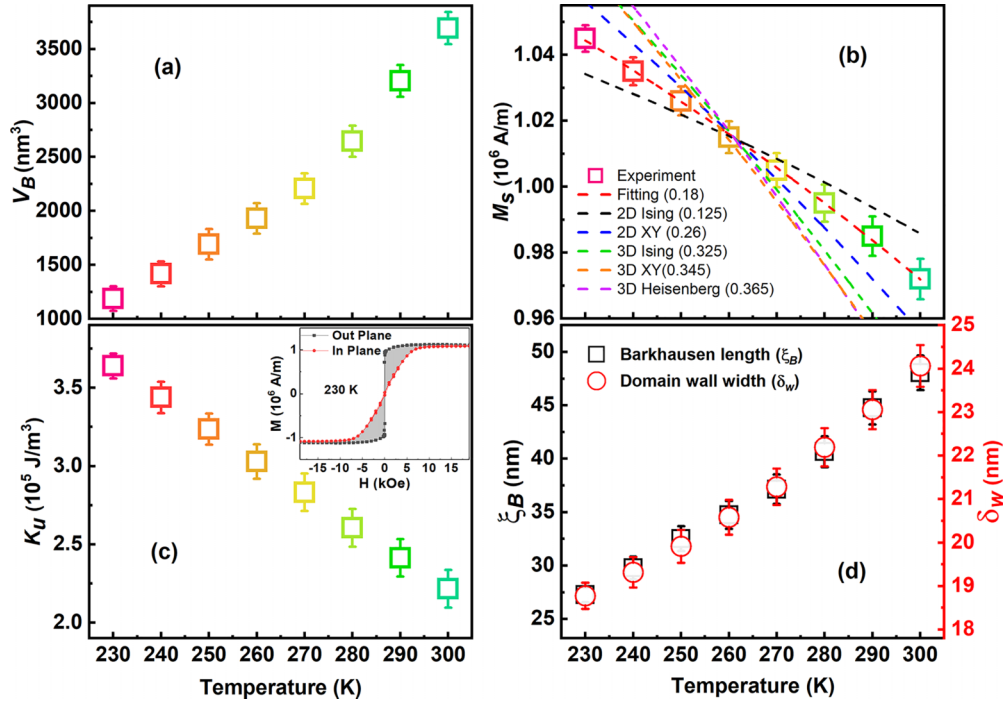


FIG. 4. (a) Barkhausen volume (V_B) at various temperatures. (b) Temperature-dependent saturation magnetization (M_s). The best fitting is with $\beta = 0.18 \pm 0.02$. Values from 2D Ising (0.125), 2D XY (0.26), 3D Ising (0.325), 3D XY (0.345), and 3D Heisenberg (0.365) models are shown as well. (c) Magnetic anisotropy (K_u) at different temperatures. Inset: Comparison of hysteresis area between hard axis (in-plane) and easy axis (out-plane) hysteresis loop at 230 K. (d) Barkhausen length (ξ_B) and domain-wall width (δ_w) with respect to the temperature.

The fitted values of V_B from Eq. (2) at each temperature are plotted in Fig. 4(a). Very interestingly, V_B increases significantly from 1251 to 3719 nm³ for the variation of temperature from 230 to 300 K. At elevated temperature, the thermal energy facilitates magnetic moment to overcome the energy barrier and reverse their magnetization. Therefore, possible origin of substantial increase of V_B in the relatively narrow temperature range could be linked to the reduction of energy barrier, as observed by the significant change of H_C in Fig. 1(b). This is because H_C serves as representation of the strength of the magnetic field (H) needed to overcome the energy barrier (E_b) and reverse the magnetization. In case of uniaxial perpendicular anisotropy film, the magnetic energy is expressed as $E = K_u V \sin^2 \theta - \mu_0 M_s H V \cos(\varphi - \theta)$, where θ and φ are the angle of magnetization and external applied field (H) from the easy axis, respectively. V is the volume of magnetic reversal [46]. Then, the energy barrier is

$$E_b = E_{\max} - E_{\min} = K_u V \left(1 + \frac{\mu_0^2 M_s^2 H^2}{4K_u^2} \right) - \mu_0 M_s H V. \quad (3)$$

Thus, temperature-dependent M_s and K_u behaviors should be examined to explain the temperature-dependent V_B behavior.

In Fig. 4(b), temperature-dependent M_s is plotted, with fitting by Eq. (4):

$$M_s(T) = M_0 \left(1 - \frac{T}{T_c} \right)^\beta, \quad (4)$$

where M_0 represents zero-temperature magnetic moment, T_c is Curie temperature, and β is the critical exponent related

to the universality class [9]. The best fitting of β exponent is found to be 0.18 ± 0.04 , again close to the theoretical prediction ($\beta = 0.125$) for the 2D Ising model, while β values for the 2D XY, 3D Ising, 3D XY, and 3D Heisenberg models are 0.26, 0.325, 0.345, and 0.365, respectively [9,47,48], suggesting that the magnetization behavior is 2D Ising-like. Furthermore, K_u at each temperature is measured, as in Fig. 4(c), by quantitative comparison of hysteresis loop area along the easy- and hard axis, as seen in the inset of the figure for the case of 230 K. It is noteworthy that a relative degree of reduction of K_u ($\sim 39\%$) is substantially larger compared to the case of M_s ($\sim 7\%$), implying a significant role of K_u in determination of V_B . Considering the present sample is two-dimensional film, Barkhausen length (ξ_B) can be determined by $\xi_B = (V_B/t_{\text{CoFeB}})^{1/2}$, where t_{CoFeB} is the film thickness.

On the other hand, it has long been believed that the ξ_B is linked to the exchange-length scale, which is approximated as the DW width, δ_w . Since $\delta_w = \pi \sqrt{A_{\text{ex}}/K_u}$, with the exchange stiffness constant A_{ex} of CoFeB film (13 pJ/m) [49], temperature-dependent ξ_B and δ_w are compared as demonstrated in Fig. 4(d). ξ_B increases with respect to the temperature from 27.9 to 48.2 nm, as previously observed [25,26], while δ_w increases from 18.7 to 24.0 nm. Note that the ξ_B is determined from v fitting while δ_w is determined from K_u measurement. Interestingly, the temperature-dependent behaviors of ξ_B and δ_w are directly correlated in the temperature range, where the 2D Ising-like universality is sustained. Our investigation based on direct domain observation reveals that a thermal agitation reducing the K_u effectively reduces the E_b , and thus, directly controls the Barkhausen length scale in the

temperature range for the case of single-domain 2D Ising-like system.

In conclusion, we report our experimental verification of the proof of principle that the temperature-dependent Barkhausen volume is directly linked to the temperature-dependent uniaxial perpendicular magnetic anisotropy, while the single-domain and the 2D Ising-like features of two-dimensional ferromagnetic film are persistent. A simplistic model system of CoFeB film with perpendicular magnetic anisotropy is carefully maintained, where the scaling behaviors of hysteresis area and saturation magnetization are quantitatively analyzed, together with direct domain pattern observations. Our work will provide an experimental founda-

tion for further understanding of statistical nature of DW dynamics based on investigation of microscopic nature of the interface.

This research was supported by the Commercialization Promotion Agency for R&D Outcomes (COMPA) funded by the Ministry of Science and ICT (MSIT) (Grant No. 1711198544, Development of analytical instrumentation for electromagnetics/optics/thermal characteristics under extreme environment). This research was also supported by the National Research Foundation of Korea (NRF) (Grant No. RS-2023-00250178). C.-Y.Y. and E.B. were supported by NRF (Grant No. 2021M3F3A2A01037525).

-
- [1] O. Portmann, A. Vaterlaus, and D. Pescia, An inverse transition of magnetic domain patterns in ultrathin films, *Nature (London)* **422**, 701 (2003).
- [2] I. Tudosa, C. Stamm, A. B. Kashuba, F. King, H. C. Siegmann, J. Stöhr, G. Ju, B. Lu, and D. Weller, The ultimate speed of magnetic switching in granular recording media, *Nature (London)* **428**, 831 (2004).
- [3] N. Saratz, U. Ramsperger, A. Vindigni, and D. Pescia, Irreversibility, reversibility, and thermal equilibrium in domain patterns of Fe films with perpendicular magnetization, *Phys. Rev. B* **82**, 184416 (2010).
- [4] J. Brooke, T. F. Rosenbaum, and G. Aeppli, Tunable quantum tunnelling of magnetic domain walls, *Nature (London)* **413**, 610 (2001).
- [5] N. Frangieh, G. Accary, D. Morvan, S. Méradji, and O. Bessonov, Wildfires front dynamics: 3D structures and intensity at small and large scales, *Combust. Flame* **211**, 54 (2020).
- [6] A. S. Balankin, R. G. Paredes, O. Susarrey, D. Morales, and F. C. Vacio, Kinetic roughening and pinning of two coupled interfaces in disordered media, *Phys. Rev. Lett.* **96**, 056101 (2006).
- [7] V. J. Emery and S. A. Kivelson, Importance of phase fluctuations in superconductors with small superfluid density, *Nature (London)* **374**, 434 (1995).
- [8] X. Gabaix, P. Gopikrishnan, V. Plerou, and H. E. Stanley, A theory of power-law distributions in financial market fluctuations, *Nature (London)* **423**, 267 (2003).
- [9] H. E. Stanley, *Introduction to Phase Transitions and Critical Phenomena* (Clarendon Press, Oxford, 1971), pp. 109–133.
- [10] D.-H. Kim, S.-B. Choe, and S.-C. Shin, Direct observation of Barkhausen avalanche in Co thin films, *Phys. Rev. Lett.* **90**, 087203 (2003).
- [11] G. Meier, M. Bolte, R. Eiselt, B. Krüger, D.-H. Kim, and P. Fischer, Direct imaging of stochastic domain-wall motion driven by nanosecond current pulses, *Phys. Rev. Lett.* **98**, 187202 (2007).
- [12] M.-Y. Im, P. Fischer, D.-H. Kim, K.-D. Lee, S.-H. Lee, and S.-C. Shin, Direct real-space observation of stochastic behavior in domain nucleation process on a nanoscale, *Adv. Mater.* **20**, 1750 (2008).
- [13] J. M. D. Coey, *Magnetism and Magnetic Materials* (Cambridge University Press, Cambridge, MA, 2009).
- [14] Y. Yu, L. Tauxe, and B. M. Moskowitz, Temperature dependence of magnetic hysteresis: Magnetic hysteresis, *Geochem. Geophys. Geosystems* **5**, 1 (2004).
- [15] C. Zener, Classical theory of the temperature dependence of magnetic anisotropy energy, *Phys. Rev.* **96**, 1335 (1954).
- [16] D.-T. Quach, T.-D. Chu, D.-T. Ngo, and D.-H. Kim, Correlation of hysteresis loop and domain structure of CoFeB/Pd multilayer at various temperatures, *Phys. B: Condens. Matter* **577**, 411822 (2020).
- [17] L. He and C. Chen, Effect of temperature-dependent shape anisotropy on coercivity for aligned Stoner-Wohlfarth soft ferromagnets, *Phys. Rev. B* **75**, 184424 (2007).
- [18] P. J. Metaxas, J. P. Jamet, A. Mougin, M. Cormier, J. Ferré, V. Baltz, B. Rodmacq, B. Dieny, and R. L. Stamps, Creep and flow regimes of magnetic domain-wall motion in ultrathin Pt/Co/Pt films with perpendicular anisotropy, *Phys. Rev. Lett.* **99**, 217208 (2007).
- [19] W. Wernsdorfer, E. B. Orozco, K. Hasselbach, A. Benoit, B. Barbara, N. Demoncy, and D. Mailly, Experimental evidence of the Néel-Brown model of magnetization reversal, *Phys. Rev. Lett.* **78**, 1791 (1997).
- [20] J. Gorchon, S. Bustingorry, J. Ferré, V. Jeudy, A. B. Kolton, and T. Giamarchi, Pinning-dependent field-driven domain wall dynamics and thermal scaling in an ultrathin Pt/Co/Pt magnetic film, *Phys. Rev. Lett.* **113**, 027205 (2014).
- [21] V. Jeudy, A. Mougin, S. Bustingorry, W. Savero Torres, J. Gorchon, A. B. Kolton, A. Lemaître, and J.-P. Jamet, Universal pinning energy barrier for driven domain walls in thin ferromagnetic films, *Phys. Rev. Lett.* **117**, 057201 (2016).
- [22] R. Diaz Pardo, W. Savero Torres, A. B. Kolton, S. Bustingorry, and V. Jeudy, Universal depinning transition of domain walls in ultrathin ferromagnets, *Phys. Rev. B* **95**, 184434 (2017).
- [23] S.-B. Choe and S.-C. Shin, Observation of unequal activation volumes of wall-motion and nucleation processes in Co/Pd multilayers, *Phys. Rev. Lett.* **86**, 532 (2001).
- [24] A. Kirilyuk, J. Ferré, V. Grolier, J. P. Jamet, and D. Renard, Magnetization reversal in ultrathin ferromagnetic films with perpendicular anisotropy, *J. Magn. Magn. Mater.* **171**, 45 (1997).
- [25] A. Enders, D. Repetto, D. Peterka, and K. Kern, Temperature dependence of the magnetism in Fe/Cu (001), *Phys. Rev. B* **72**, 054446 (2005).

- [26] A. Kirilyuk, J. Ferre, and D. Renard, Temperature effects on domain wall dynamics in ultrathin ferromagnetic films, *IEEE Trans. Magn.* **29**, 2518 (1993).
- [27] D.-T. Ngo, D.-T. Quach, Q.-H. Tran, K. Møhave, T.-L. Phan, and D.-H. Kim, Perpendicular magnetic anisotropy and the magnetization process in CoFeB/Pd multilayer films, *J. Phys. Appl. Phys.* **47**, 445001 (2014).
- [28] C. De Julián Fernández, Influence of the temperature dependence of anisotropy on the magnetic behavior of nanoparticles, *Phys. Rev. B* **72**, 054438 (2005).
- [29] A. López-Ortega, E. Lottini, C. D. J. Fernández, and C. Sangregorio, Exploring the magnetic properties of cobalt-ferrite nanoparticles for the development of a rare-earth-free permanent magnet, *Chem. Mater.* **27**, 4048 (2015).
- [30] M.-C. Tsai, C.-W. Cheng, C. C. Tsai, and G. Chern, The intrinsic temperature dependence and the origin of the crossover of the coercivity in perpendicular MgO/CoFeB/Ta structures, *J. Appl. Phys.* **113**, 17C118 (2013).
- [31] C. Fowley, N. Decorde, K. Oguz, K. Rode, H. Kurt, and J. M. D. Coey, Perpendicular magnetic anisotropy in CoFeB/Pd bilayers, *IEEE Trans. Magn.* **46**, 2116 (2010).
- [32] S. A. Majetich, T. Wen, and O. T. Mefford, Magnetic nanoparticles, *MRS Bull.* **38**, 899 (2013).
- [33] E. C. Stoner and E. P. Wohlfarth, A mechanism of magnetic hysteresis in heterogeneous alloys, *Philos. Trans. R. Soc. London* **240**, 599 (1948).
- [34] R. H. Victora, Predicted time dependence of the switching field for magnetic materials, *Phys. Rev. Lett.* **63**, 457 (1989).
- [35] J. Garcia-Otero, A. J. Garcia-Bastida, and J. Rivas, Influence of temperature on the coercive field of non-interacting fine magnetic particles, *J. Magn. Magn. Mater.* **189**, 377 (1998).
- [36] C. P. Steinmetz, On the law of hysteresis, *Proc. IEEE* **72**, 197 (1984).
- [37] Z. Huang, F. Zhang, Z. Chen, and Y. Du, Dynamic transition and hysteresis scaling in Heisenberg ferromagnet, *Eur. Phys. J. B* **44**, 423 (2005).
- [38] B. C. Choi, W. Y. Lee, A. Samad, and J. A. C. Bland, Dynamics of magnetization reversal in thin polycrystalline Ni₈₀Fe₂₀ films, *Phys. Rev. B* **60**, 11906 (1999).
- [39] D. Handoko, S.-H. Lee, K. Min Lee, J.-R. Jeong, and D.-H. Kim, Comparison of hysteresis loop area scaling behavior of Co/Pt Multilayers: Discrete and continuous field sweeping, *J. Magn. Magn. Mater.* **351**, 82 (2014).
- [40] P. J. Van Der Zaag, New views on the dissipation in soft magnetic ferrites, *J. Magn. Magn. Mater.* **196**, 315 (1999).
- [41] M. Acharyya and B. K. Chakrabarti, Response of Ising systems to oscillating and pulsed fields: Hysteresis, Ac, and pulse susceptibility, *Phys. Rev. B* **52**, 6550 (1995).
- [42] A. L. Barabási and H. E. Stanley, *Fractal Concepts in Surface Growth* (Cambridge University Press, Cambridge, 1995).
- [43] D.-H. Kim, Y.-C. Cho, S.-B. Choe, and S.-C. Shin, Correlation between fractal dimension and reversal behavior of magnetic domain in Co/Pd nanomultilayers, *Appl. Phys. Lett.* **82**, 3698 (2003).
- [44] Junyeon Kim, Kab-Jin Kim, and Sug-Bong Choe, Temperature dependence of domain-wall creep in Pt/CoFe/Pt films, *IEEE Trans. Magn.* **45**, 3909 (2009).
- [45] S. Lemerle, J. Ferré, C. Chappert, V. Mathet, T. Giamarchi, and P. Le Doussal, Domain wall creep in an Ising ultrathin magnetic film, *Phys. Rev. Lett.* **80**, 849 (1998).
- [46] C. Tannous and J. Gieraltowski, The Stoner–Wohlfarth model of ferromagnetism, *Eur. J. Phys.* **29**, 475 (2008).
- [47] Z. Li, X. Wei, and Y. Guo, Magnetic critical behavior of the van der Waals Fe₃GeTe₂ crystal with near room temperature ferromagnetism, *Sci. Rep.* **10**, 15345 (2020).
- [48] P. Borisov and W. Kleemann, Exchange bias and ferromagnetic coercivity in heterostructures with antiferromagnetic Cr₂O₃, *J. Appl. Phys.* **110**, 033917 (2011).
- [49] G.-M. Choi, Exchange stiffness and damping constants of spin waves in CoFeB films, *J. Magn. Magn. Mater.* **516**, 167335 (2020).